Jiao, R., Yang, R., Yuan, X. (2021): Incision History of the Three Gorges, Yangtze River Constrained From Inversion of River Profiles and Low-Temperature Thermochronological Data. - Journal of Geophysical Research: Earth Surface, 126, 3, 2020JF005767.

https://doi.org/10.1029/2020JF005767

JGR Earth Surface

RESEARCH ARTICLE
10.1029/2020JF005767

Incision History of the Three Gorges, Yangtze River Constrained From Inversion of River Profiles and Low-Temperature Thermochronological Data

Ruohong Jiao[1], **Rong Yang**[2], **and Xiaoping Yuan**[3]

[1]School of Earth and Ocean Sciences, University of Victoria, Victoria, Canada, [2]School of Earth Sciences, Zhejiang University, Hangzhou, China, [3]Helmholtz Centre Potsdam, GFZ German Research Centre for Geosciences, Potsdam, Germany

Key Points:

- River incision history is modeled using topographic and published (U-Th)/He data
- Inversion of the data suggests accelerated incision rate since the early Miocene
- Gorge incision rate decreased during the Pliocene due to the declined monsoonal rainfall

Correspondence to:
R. Jiao,
rjiao@uvic.ca

Citation:
Jiao, R., Yang, R., & Yuan, X. (2021). Incision history of the Three Gorges, Yangtze River constrained from inversion of river profiles and low-temperature thermochronological data. *Journal of Geophysical Research: Earth Surface*, *126*, e2020JF005767. https://doi.org/10.1029/2020JF005767

Received 28 JUN 2020
Accepted 8 JAN 2021

Abstract We reconstruct the incision history of bedrock rivers based on inverse modeling of the long profile of a river channel and the low-temperature thermochronological data. Our approach first infers an erodibility-dependent incision history through a linear inversion of the channel elevations of the river. Then to calibrate the reconstructed incision history in the geological timescale, we constrain the erosional efficiency by optimizing the erosion process of the river catchment using a Bayesian analysis, such that the exhumation and cooling paths of bedrocks in the catchment conform to the observed thermochronological ages. We apply this approach to estimate the incision history of the Three Gorges, Yangtze River in East Asia. We modeled the incision histories of three tributaries on the mainstem Yangtze River near the eastern end of the Three Gorges area, assuming that the gorge incision was driven by increased upstream drainage area of the Upper Yangtze (Scenario 1) or local tectonic uplift (Scenario 2). The results of both scenarios suggest an early Miocene onset of the incision of Three Gorges, that is, 18 ± 6 Ma or 21 ± 4 Ma, respectively. During the Pliocene, our models suggest a significant decrease in the gorge incision rate. By comparing the estimated gorge incision history to the late Cenozoic denudation of the eastern Tibetan Plateau and the regional climate change, we suggest that the incision of the Three Gorges has been heavily affected by the development of the Upper Yangtze River and the East Asian monsoon.

1. Introduction

As the longest river in Asia, development of the Yangtze River (Figure 1) was a major reorganization of the river networks in East Asia, and has played an important role in the evolution of the region's topography and landscape. During the Cenozoic, the collision between the Indian and Eurasian Plates led to the rise of the Tibetan Plateau (Rowley & Currie, 2006; Wang et al., 2008), which created the current east-tilting topography of East Asia. Previous studies suggest that this marked reshaping of the topography rearranged the drainage networks of the large rivers originating on the Tibetan Plateau, including the Upper Yangtze River (Clark et al., 2004; Clift et al., 2006; Zheng , 2015). These studies hypothesized that the Upper Yangtze River used to flow southwards and drain into the South China Sea through a path parallel to the Mekong River, for example, the paleo-Red River (Clift et al., 2006). In line with this hypothesis, some studies (e.g., Clark et al., 2004; Richardson et al., 2010) further suggest a reversal of the river flow direction in the Sichuan Basin (Figure 1b): prior to the connection between the Upper and Middle Yangtze River, rivers in the Sichuan Basin used to drain westwards, joining the western part of the Upper Yangtze River before flowing toward the South China Sea. This hypothesis predicts a paleo-drainage divide on the eastern margin of the Sichuan Basin, which separated the west- and east-flowing drainage systems. Therefore, to test the above hypothesis about the evolution of the Yangtze River, constraining the incision history of the potential paleo-drainage divide between the Upper and Middle Yangtze is crucial.

On the eastern margin of the Sichuan Basin, several mountain ranges from high topography, including the Daba Shan, Wu Shan, and Xuefeng Shan (Figure 1b), which present as the most likely barriers between large drainage systems. These mountains formed as products of the collision between the North China and Yangtze Cratons during the Mesozoic (Li et al., 2017; Wang et al., 2003), and no evidence indicates a significant orogenic process in the area during the Cenozoic (Hu et al., 2006). Across the mountains, the

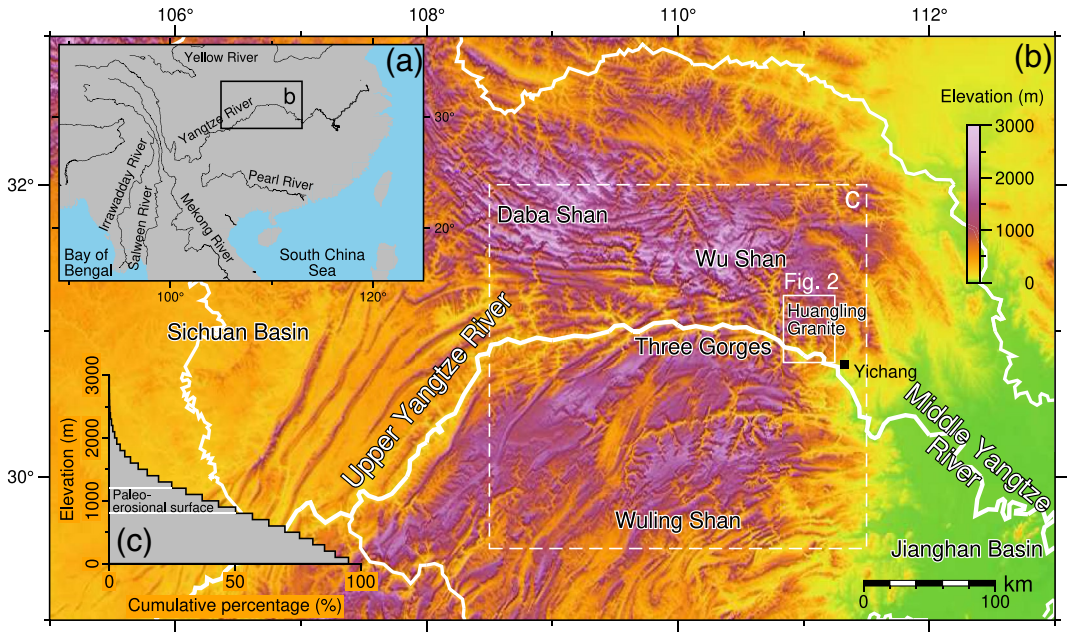

Figure 1. (a) Map showing the courses of major rivers in East Asia. Box shows the location of (b). (b) Topographic map of the Three Gorges and adjacent area. Note the high mountains between the Upper and Middle Yangtze River. White lines represent the courses of Yangtze River and its main tributaries. Box of solid line indicates the location of Figure 2. (c) Hypsometric curve for the area inside of the box of the dashed line in (b).

Sichuan Basin and alluvial plains in East China are connected through a series of narrow and deep valleys surrounded by high-relief cliffs, known as the Three Gorges (Figure 1b). While the elevation of the main channel of the Yangtze River decreased from ~100–200 m in the Sichuan Basin to <80 m in the Three Gorges, the mean elevation of the Three Gorges region (~800 m) is significantly higher than that of the upstream Sichuan Basin (~400 m). Therefore, as the key link between the Upper and Middle Yangtze River, the incision history of the Three Gorges is an important part of the development of the river. Particularly, if the Cenozoic reversal of the Sichuan Basin drainage system existed, through-cutting of the Three Gorges could be a milestone during the formation of the Yangtze River and the evolution of the drainage systems in East Asia (Richardson et al., 2010; Zheng et al., 2013).

However, despite its importance for resolving the history of the Yangtze River, the beginning time of the incision of the Three Gorges remains under debate. Based on quartz electron spin resonance (ESR) dates of the lake deposits in the downstream Jianghan Basin (Figure 1b), Xiang et al. (2007) suggested that the Yangtze River did not flow through the Three Gorges before 0.75 Ma. By dating the fluvial deposits on the valley shoulders in the Three Gorges, Li et al. (2001) identified several postPleistocene terraces and suggested that the gorge incision started at 2.1 Ma. Using apatite fission track (AFT) and (U-Th)/He data of the bedrock samples from the eastern part of gorge region, Richardson et al. (2010) inferred an increase in the cooling rate of the Huangling Granite (Figure 1b) at ~45–40 Ma, and interpreted it as the consequence of high-erosion rate since the onset of the gorge incision. Zheng et al. (2013) suggested that the Three Gorges was cut through between 36.5 and 23 Ma, constrained by the prelate Eocene evaporite and lacustrine sediments in the Jianghan Basin and the temporally invariant zircon U-Pb age patterns of the postOligocene sediments from the further downstream Yangtze River, respectively.

Here, we present a study of the evolution of the Three Gorges, which extracts the incision timing and rate by inverse modeling both the long-profiles of rivers and the bedrock low-temperature thermochronological data. Inversion of the river profiles is based on the stream power model (Howard & Kerby, 1983; Royden & Perron, 2013) and uses current spatial distribution of the channel gradients of a river to solve for the temporal change in the uplift rate relative to the base level (Goren et al., 2014). The solution is, however, dependent on the efficiency of the river erosion, and calibrating the modeled uplift rate history in the geological time requires independent, empirical constraints on the river erosion history. Constraints

used in previous studies include basin-averaged erosion rates derived from cosmogenic ^{10}Be concentrations (e.g., Li et al., 2020) and single-site rock exhumation magnitude estimated from low-temperature thermochronological data (e.g., Fox et al., 2015; Goren et al., 2014), which cannot provide information about the spatial variation in the erosion rates. In this study, we calibrate the modeled river uplift/incision history by simultaneously reproducing multiple thermochronological ages collected from different locations in the catchment. This approach not only allows us to estimate the efficiency of the river erosion, but also acts as an independent test of the compatibility between the erosion rate distribution pattern modeled from topographic data and that estimated from low-temperature thermochronology.

The approach we use in this study is summarized as follows. Based on inversion of the long profiles of river channels using a linear method (Goren et al., 2014), we first estimate the uplift history of three tributaries relative to their outlets on the Yangtze River in the Three Gorges area, and calculate the erosion rate variation along the channels of the tributaries. The modeled uplift and erosion histories are both dependent on the erosional efficiency. Then by prescribing the parameters for the erosional efficiency and the thermal model of the crust, we are able to use the inferred river erosion history to predict the cooling paths and thermochronological ages of rock samples in the drainage area. For predicting the thermal histories, we test two end-member scenarios, in which the relative uplift is assumed to be driven by either (1) lowering of the tributaries' outlets at the mainstem Yangtze River or (2) tectonic uplift of the tributaries' catchments, respectively. Finally, for each scenario we optimize the values of prescribed model parameters and constrain the river incision history by minimizing the misfit between the predicted and observed cooling ages from the river catchment.

2. Geological, Climatic, and Geomorphic Settings

The eastern end of the Three Gorges, located in the interior of the Yangtze Craton, exposes some of the oldest rocks in South China. The area features a dome structure with the Neoproterozoic Huangling Granite (Wei et al., 2012; Figure 1b) surrounded by Precambrian and Phanerozoic (meta) sedimentary rocks (Gao et al., 2011). From the Late Jurassic to the Late Cretaceous, rocks in the area underwent two phases of strong deformation, due to the earlier convergence between the North China and Yangtze blocks and the later intracontinental compression in South China (Li et al., 2012). Since the Paleogene, the adjacent foreland basin entered a period of postorogenic extension (Shi et al., 2013), with no significant deformation documented within the Huangling Granite until the present day.

Except some metasedimentary complex exposed in the middle reach of the Baisui Brook, the substrate of the three catchments in this study is the Huangling Granite (Figure 2). Low-temperature thermochronological data and thermal history modeling suggest that the Huangling Granite experienced a period of rapid exhumation between 150 and 180 Ma (Ge et al., 2013). Based on the U-Pb ages of the detrital zircons from the sediments in the adjacent, downstream Jianghan Basin, Shen et al. (2012) suggested that the granite had already been exposed to the surface by the Late Cretaceous. In contrast, from the Cenozoic sedimentary sections downstream of the Huangling dome, Wang et al. (2014) observed no granitoid clasts in the pre-Neogene stratigraphy and suggested that the Huangling Granite has only been exposed since the late Cenozoic. Despite this dispute, it appears that at least over the late Cenozoic, the bedrocks in the three Yangtze tributaries studied here present a generally uniform lithology, and thus the bedrock erodibility is likely constant through time in most of the study areas.

Located in the Central China, the Three Gorges region is heavily affected by a monsoonal climate with intensified rainfalls during the summer (Ding, 1992). The starting time of the East Asian monsoon is still highly debated. Although earlier studies suggest an onset during the Miocene (e.g., An et al., 2001) or the latest Oligocene (e.g., Sun & Wang, 2005), a recent study based on a compilation of multiple proxies and climate modeling suggests that the annual monsoonal precipitation started during the late Paleocene–Eocene (Farnsworth et al., 2019). Therefore, we consider the climatic influence on the river incision rate unchanged over the late Cenozoic, until the Pliocene when the mean annual precipitation reduced in East Asia (Farnsworth et al., 2019; Wang et al., 2019). Climatic conditions oscillate over shorter timescales between glacial and interglacial periods, but they should have negligible impact on the long-term erosion rate (e.g., Armitage et al., 2013) and leave no significant record on the bedrock landscape (Goren, 2016)

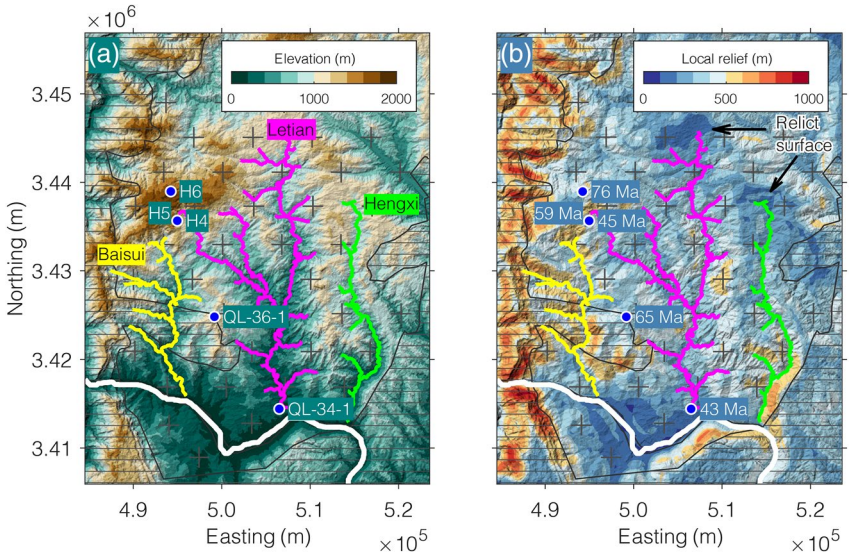

Figure 2. Maps showing (a) topography and (b) local relief (1 km^2) of the eastern end of the Three Gorges. White line depicts the mainstem of the Yangtze River, and colored lines represent three tributaries in the study area: A, yellow; B, magenta; C, green. Note the low-relief paleo-surface at the headwaters of Letian and Hengxi Brooks. Hatch fills indicate the approximate distributions of the granitoid (pluses) and metasedimentary rocks (lines) in the Huangling dome. Also shown are sample numbers (in a) and apatite (U-Th)/He ages (in b) from Hu et al. (2006) and Richardson et al. (2010).

Planation surfaces result from a long-period of regional-scale erosion and present as large areas of flat or gently tilted bedrock surfaces (Orme, 2013; Zhang, 2008). These low-relief surfaces develop at a local base level, and are eventually preserved after a base level fall or tectonic uplift. In tectonically stable regions, a planation surface can be preserved for several tens of million years after its initial formation (e.g., Guillocheau et al., 2018). In the Three Gorges area, several levels of the planation surfaces are observed. Near the mountain summits at elevations between ~1,200 and 2,000 m (Shen, 1965), the planation surfaces are away from the mainstem of the Yangtze River. These surfaces cut through the strata of ages spanning from the Cambrian to Jurassic (Xie et al., 2006), indicating that they formed no earlier than the Late Mesozoic. Below the high-level surfaces, another level of low-relief surfaces exist at elevations between ~800 and 1,200 m (Figure 1c; Xie et al., 2006), in forms of intermontane basins, plateaus, karst platforms, and low-gradient river valleys. In this study, the headwaters of both Letian and Hengxi Brooks originated on planation surfaces of this level (Figure 2b).

Due to the lack of direct constraints on the uplift histories of the low-relief surfaces, we consider two possible periods for their formation. For the first possibility, we assume that the surfaces in the Three Gorges area were uplifted during the Mesozoic. Elevated planation surfaces have been observed at many locations in the Qingling-Dabie mountain belt (Feng & Cui, 2002), which was last uplifted and exhumed by the Early Cretaceous during the collision between North China and Yangtze blocks (Dong & Santosh, 2016; Zhang et al., 1996). For example, planation surfaces exist in the eastern Dabie Shan at elevations up to >1,300 m (Rao et al., 2013), where the exhumation rate has remained low and topographic relief has decreased during the Cenozoic (Braun & Robert, 2005; Reiners et al., 2003). The Huangling Granite is located on the northern margin of the Yangtze block, and therefore the planation surface could be uplifted prior to the cessation of the North China-Yangtze collision. As the second possibility, we assume the that the planation surfaces were uplifted during the Late Cenozoic. Previous studies suggested that the bedrock mountains to the northeast of the Sichuan Basin, including the Daba Shan (Figure 1b), were uplifted and exhumed during the Late Cenozoic, as a result of the eastward propagation of the Tibetan Plateau (Tian et al., 2012; Yang et al., 2017). As an eastward continuation of the Daba Shan in space, it is possible that the Huangling Granite experienced the same period of uplift during the Cenozoic, which raised the planation surfaces to their current elevations. These two possibilities make no difference in our inversion of the catchments' uplift histories relative to the base level, but are considered as different scenarios when we estimate the paleo-topography of the river channels and model the thermal histories (Sections 3.2 and 4).

3. Inverting the River Profile for Incision History and Paleotopography

The incision of river channels below the low-relief erosional surface was driven by an increased rock uplift rate relative to the base level near their outlets. As two end-members, this relative uplift rate represents either (1) the difference between rock uplift and lowering of the base level at the outlet, that is, in our case the elevation of the mainstem Yangtze River, or (2) the tectonic uplift relative to a fixed base level. Assuming this uplift rate is spatially uniform in the catchments, we estimate the temporal variation of the relative uplift rate (u) by analyzing the river profiles using the linear inversion method of Goren et al. (2014).

3.1. Method

According to the stream power incision model (Howard & Kerby, 1983; Whipple & Tucker, 1999), the rate of elevation change in bedrock river channels can be predicted as the difference between rock uplift rate and fluvial incision rate, using the equation:

$$\frac{\partial z(t,x)}{\partial t} = u(t,x) - K(t,x)A(x)^m\left(\frac{\partial z(t,x)}{\partial x}\right)^n, \tag{1}$$

where z is the channel elevation, t is the time, x is the along-channel distance from the outlet, u is the uplift rate relative to the base level, K is the bedrock erodibility, A is the upstream drainage area that is used to approximate the discharge, and m and n are the area and slope exponents, respectively. Royden and Perron (2013) provided a solution for Equation (1), the linear form ($n = 1$) of which was used by Goren et al. (2014) to invert for tectonic uplift history from fluvial river profiles. By assuming a spatially uniform uplift rate (i.e., $u(t) = u$), Goren et al. (2014) presented the solution of the topography as

$$z(t,x) = \int_{t-\tau(x)}^{t} u(t')dt', \tag{2}$$

where t' is the integration parameter, and $\tau(x)$ is the time required for the signal of uplift rate change to migrate to x, expressed as

$$\tau(x) = \int_0^x \frac{dx'}{KA(x')^m}, \tag{3}$$

in which x' is the integration parameter. To remove the dependence of τ on K, Goren et al. (2014) transformed Equation (2) to

$$z(t^*,x) = \int_{t^*-\chi(x)}^{t^*} u^*(t')dt', \tag{4}$$

by imposing three K-dependent parameters

$$\chi = A_0^m K\tau, u^* = \frac{u}{KA_0^m} \text{ and } t^* = KA_0^m t, \tag{5}$$

where A_0 is an imposed area value to scale the drainage area, and χ is a measure of the transient state of the river profile introduced by Perron and Royden (2013).

To reconstruct the paleo-topography, we follow the simplification as in Fox (2019), which assumes that topography was in steady state prior to an uplift rate change. By discretizing the river profile into a limited number (N) of pixels, the present-day ($t^* = 0$) elevation of pixel i can be expressed in a discrete form (Fox, 2019; Goren et al., 2014) as

$$z_i = \sum_{j=1}^{i}(\chi_j - \chi_{j-1})u_j^*, \tag{6}$$

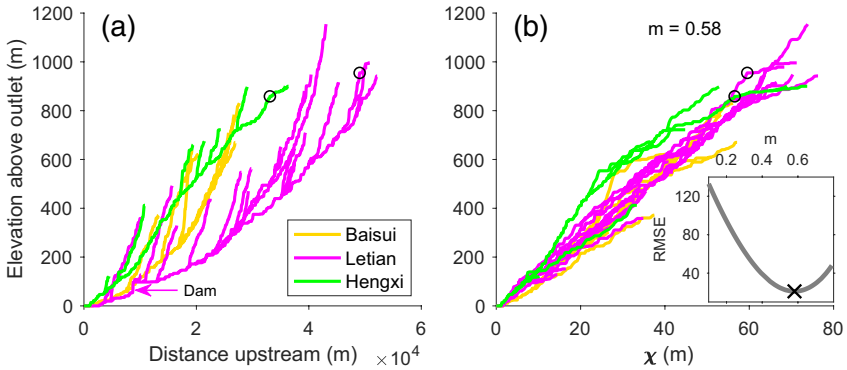

Figure 3. (a) Long-profiles of the three rivers in the study area for channels with an upstream drainage area >4.5 km^2. Topographic data are from the ASTER Global Digital Elevation Model (30 m resolution). (b) χ-elevation plots of the river channels using $m = 0.58$ and $A_0 = 1$ km^2. Inset shows the scattering of the χ-plots with different values of m. ASTER, Advanced Spaceborne Thermal Emission and Reflection Radiometer.

in which the pixels are ordered upstream from the outlet such that $\chi_0 = 0$. Then by dividing the uplift history into a small number (q) of intervals ($q \ll N$), solving u^* becomes an overdetermined inverse problem (Goren et al., 2014), for which we optimize using a linear least-squares method (with the *lsqnonneg* function in the MATLAB software). Finally, paleo-topography of the river channels relative to the base level as a function of t^* can be calculated using Equation (4). See Goren et al. (2014) for a detailed description of the method.

We extract the elevation data of the Baisui, Letian, and Hengxi Brooks from the Advanced Spaceborne Thermal Emission and Reflection Radiometer (ASTER) Global Digital Elevation Model (30 m spatial resolution). To calculate the χ values in Equation (6), we use the elevations of their outlets at the Yangtze River as the base level, and parameter values of $A_0 = 10^6$ m^2 and $m = 0.58$. The value of m, the drainage area exponent in Equation (1), is optimized by minimizing the scattering of the χ-plots such that the pixels with the same χ values are at similar elevations (Figure 3b). We solve Equation (6) for each of the three rivers in the study area separately.

3.2. Results

Inversion results are summarized in Figure 4. Our experiments with different values of the number of intervals indicate that a good fit between observed and predicted present-day topography is achieved using >8 intervals for Baisui and Hengxi Brooks, and >22 for Letian (Figure 4d). The solutions for the Letian and Hengxi Brooks suggest an increase in the incision rates prior to $t^* = 60$ (Figure 2b and 2c). In contrast, the incision history of the Baisui Brook is solved for a shorter time period, and no dramatic change in the erosion rate is shown during the model period (Figure 4a).

The estimated paleo-topography of the channels of the Letian and Hengxi Brooks show that due to its larger drainage area, the long profile of the Letian Brook adapts more quickly to the increased incision rate than that of the Hengxi Brook (Figure 5). We calibrate the reconstructed paleo-topography by assuming two possible uplift periods of the planation surfaces (Section 2). In Scenario 1, the planation surfaces are assumed to have uplifted during the Mesozoic, and therefore they have remained at the same elevation over the Cenozoic (Figure 5a and 5b). This end-member scenario represents the case that the increase in incision rate was driven by lowering of the rivers' outlets at the mainstem Yangtze River. Thus the mean elevation of the catchments decreased, and the relative uplift u represents the difference between the rock uplift of the channels and the lowering (negative uplift) of the mainstem Yangtze River. In Scenario 2, the elevation of the rivers' base level has remained constant over the late Cenozoic, and the increased incision was entirely caused by the accelerated block uplift of the catchments (Figure 5c and 5d). In this case, the mean elevation of the catchments increased, and the relative uplift rate u represents the rock uplift rates of the Huangling Granite relative to the fixed base level.

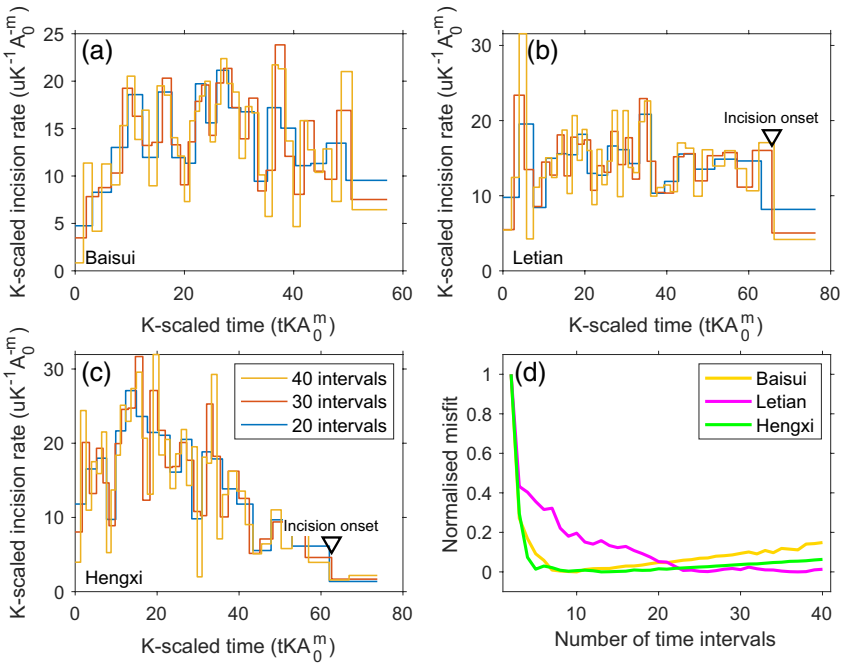

Figure 4. (a–c) Inferred incision (relative uplift) rate histories of the rivers using different numbers of time intervals (N). Triangles point to the onset of rapid incision at the Letian and Hengxi Brooks. Note that the lengths of time intervals in each model generally increase from the present-day toward the past, reflecting the upstream increase of the χ gradient from the outlet to the headwaters. In Letian and Hengxi Brooks, the slow incision rates prior to the rapid incision onset correspond to the low-relief planation surface preserved at the rivers' sources. (d) Normalized misfit as a function of number of time intervals. Optimal results are achieved when $N > 25$.

4. Constraining the Erosional Efficiency *K* Using (U-Th)/He Ages

To constrain the onset timing and rate of the incision of the Three Gorges in natural dimensions, we use apatite (U-Th)/He (AHe) ages (Figure 2) reported in the catchment of the Letian Brook (Hu et al., 2006; Richardson et al., 2010) to estimate the value of bedrock erodibility K. We do not use the ages reported from the nearby Baisui Brook, to avoid the potential bias on the estimated incision history introduced by the variable lithology in the catchment area (Figure 2). Two different erosion models are constructed according to the incision scenarios described above, respectively.

4.1. Method

For a given erosional efficiency, K, we can construct a forward model that simulates the erosion and cooling process of all samples and predicts their AHe ages. Then we estimate the values of K and other unknown parameters using a Bayesian approach, by optimizing the fit between the predicted and observed AHe ages. For each age, we build an erosion model based on the elevation history of a channel pixel extracted from the inferred paleo-topography of the river profile (Figure 5). For a sample located on the hillslope, we assume that its elevation relative to the nearest channel pixel has remained constant.

Scenario 1 assumes a stationary tectonic setting, and therefore the tectonic uplift rate has remained constant throughout the model, which is equal to the rock uplift and erosion rates when the landscape was in the steady-state condition prior to the beginning of the gorge incision, that is, u during the oldest model interval (Figure 4b). In Scenario 2, the base level is fixed, and the tectonic uplift rate varies temporally, which is equal to u during each time interval. For both scenarios, the erosion history of a sample can be reconstructed by combining its topographic and tectonic uplift histories.

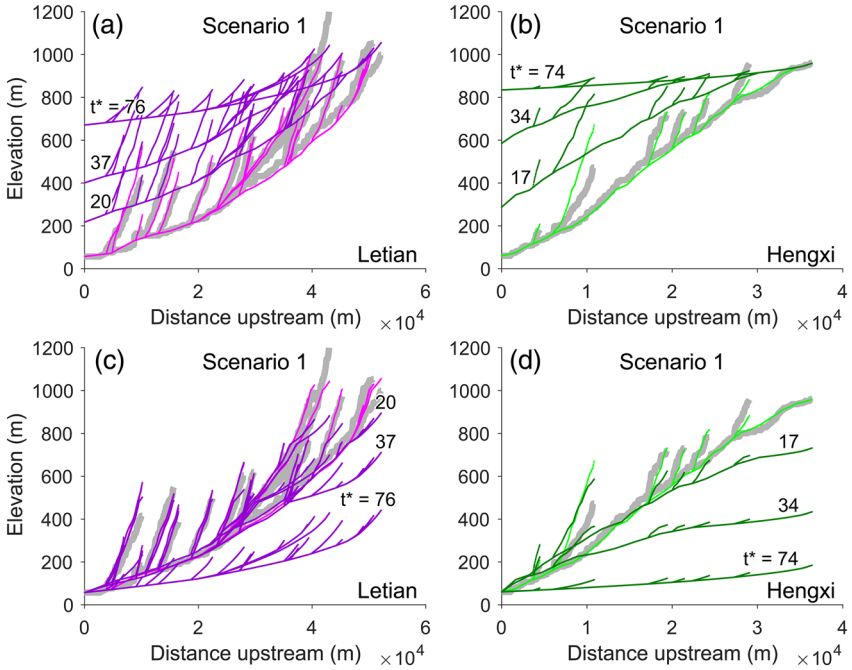

Figure 5. Calculated paleo-topography of Letian and Hengxi Brooks with models using 30 time intervals. Scenarios 1 and 2 assume fixed elevations for the low-relief planation surface and base level, respectively. Dark-colored lines indicate the modeled paleo-topography, from upper to lower, at the 30th, 20th, and 10th interval from the present, respectively. Note the oldest (uppermost) profile represents the paleo-topography prior to the incision of the erosional surface. Light colored line depicts the predicted present-day topography, and gray the observed river profile. *K*-scaled ages (t^*) of the paleo-topography are also indicated.

To build the cooling history, we prescribe a one dimensional thermal model using the parameters listed in Table 1. The parameters are chosen to approximate the 20°C/km geothermal gradient estimated in the study area (Yuan et al., 2006). We compute the thermal history by solving the heat advection-diffusion equation

$$\frac{\partial T}{\partial t} = -v\frac{\partial T}{\partial h} + \kappa\frac{\partial^2 T}{\partial h^2}, \tag{7}$$

where v is the rock uplift rate, κ is the thermal diffusivity, T is the temperature, and h is the vertical position relative to the model base. Based on Equation (5) in Scenario 1, v is constant and calculated as $v = u_q^* K A_0^m$ (q is the index of the oldest time interval); in Scenario 2, v is temporally variable and $v_j = u_j^* K A_0^m$ (j is the index of each time interval).

Table 1
Parameters Used in Thermal Model

Parameter (unit)	Value
Thickness from model base to sea level (km)	20
Number of points in the vertical direction (km)	21
Thermal diffusivity (km^2/Myr)	25
Atmospheric lapse rate (°C/km)	4
Sea-level temperature (°C)	25
Basal temperature (°C)	425

Note. These are typical values for a thermo-kinematic model (e.g., Braun et al., 2012), and are chosen to approximate the 20°C geothermal gradient in the study area (Yuan et al., 2006). Note that model topographic histories differ between Scenario 1 and Scenario 2 (Figure 5).

Equation (7) is solved at time steps of 0.1 Myr, and the temperature history of a sample is tracked according to its depth. From the thermal history, we predict the sample's AHe age using the helium diffusion model of Farley (2000). To simulate an age that is partially reset by the gorge incision, we impose an initial age, Age_0, for the thermal history model. Like the erodibility K, the value of Age_0 is also sampled by the inversion. For each forward model, we compare the computed ages of all samples and the observed data using the log-likelihood function

$$log(L) = -\sum_{i=1}^{N_a}\left[\frac{\ln(2\pi)}{2} + \ln(\sigma_i) + 0.5\left(\frac{p_i - o_i}{\sigma_i}\right)^2\right], \tag{8}$$

where p_i and o_i are the predicted and observed ages for grain age i, respectively, σ_i is the uncertainty of the observation, and N_a is the total number

of observed ages. We optimize the forward model by sampling the values of K and Age_0 using a Markov Chain Monte Carlo method (Goodman & Weare, 2010). During the inversion, the erodibility K is sampled in the range of $[10^{-10}, 10^{-8}]$ $m^{-0.16}$/yr on the logarithmic scale, that is, $\log(K)$ in the range of $[-10, -8]$. The value of Age_0 is sampled in the range of [100, 60] Ma, which corresponds to the time of the last rapid exhumation of the Huangling Granite (Ge et al., 2013; Hu et al., 2006).

4.2. Results

We tested the thermal history modeling using uplift models of the Letian Brook with different number of time intervals, but the results appear to be insensitive to the number of time intervals. This is because all models with >20 time intervals yield a similar pattern of uplift rates, and their accumulated exhumation magnitudes over the model period are all equal (Figure 5a and 5c). Therefore, here we only present the results based on the uplift model of the Letian Brook with 30 time intervals (Figure 4b). For each of the two model scenarios, we sampled a total of 60,000 forward models in the parameter space, with the first 25% discarded as burn-in (Figure 6a and 6c). The models under the two scenarios yield very similar results, both suggesting that reasonable fits to the data are obtained with $\log(K)$ in the range of $[-9.4, -8.7]$. The models are less sensitive to the initial cooling age (Age_0) of the rocks, and any value in the sampled space is acceptable. For Scenario 1, $\log(K)$ and Age_0 of the best-fit model are around −8.9 and 73.6 Ma, respectively, whereas for Scenario 2 the two parameters are around 9.0 and 72.9 Ma, respectively. For both scenarios, the best-fit models predict a wide range of AHe ages (36–66 Ma), consistent with the dispersion of observed ages from the catchment of the Letian Brook (Figure 7).

The results suggest that the current thermochronological ages are not sensitive enough to distinguish between the two scenarios of gorge incision. The cooling ages are older than our inferred time when the incision rates increased at the Yangtze River, suggesting that carving of the Three Gorges has not completely removed the fossil AHe partial retention zone. In both topographic scenarios tested, the predicted ages show a positive correlation with elevation, because (1) a higher sample was at a shallower position in the partial retention zone, and (2) the knickpoint, where the erosion rate starts to increase, generated at the Yangtze River took longer time to propagate to higher locations (Figure 8).

5. Discussion

5.1. Erosion History in the Eastern Three Gorges Area

The incision models of the Letian and the Hengxi Brooks predict a marked increase in the incision rate at $t^* = 66$ or $t^* = 62$, respectively. We suggest that this change in incision rate marks the onset of incision in the eastern Three Gorges, which led to a significant base level fall of the Letian and Hengxi Brooks. This change in incision rate is recorded on the long profiles of the two rivers as the knickpoints below the planation surface near their headwaters (Figures 2b and 3). The low-relief planation surface is not preserved in the catchment of the Baisui Brook. In turn, the χ dimension of the Baisui Brook is shorter than that of the other two rivers, and therefore has only preserved the incision history after the onset of gorge incision. Using the K values sampled during the inversion of the AHe ages, we can estimate the age of the initial gorge incision using $t = t^* / K / A_0^m$ (derived from Equation 5). For the two tested end-member scenarios, our calculation suggests onset of the gorge incision at 17.9 ± 6.3 Ma or 21.0 ± 4.2 Ma (mean ± 1σ range), respectively (Figure 6).

We are also able to constrain the change in the erosion rates of the rocks in the river catchment (Figure 8). The models of the two scenarios yield very similar results, both suggesting <0.02 km/Myr erosion rate of the Huangling Granite for the early part of the Cenozoic. Since the gorge incision started, the predicted bedrock erosion rates of Letian Brook increased to ~0.04–0.08 km/Myr near its outlet on the Yangtze River. The accelerated erosion has removed rocks of a total thickness of <1 km, which is not enough to reset the AHe ages at the present-day surface. The locus of increased erosion rates expanded upstream gradually, marked by the headward retreat of the knickpoint associated with the incision onset, which is now located at ~950 m-higher above the outlet (Figure 3). The low-relief surface at the headwaters is still eroded at ~0.02 km/Myr, not yet affected by the deep incision of the gorge (Figure 8e). Assuming that the erodibility K

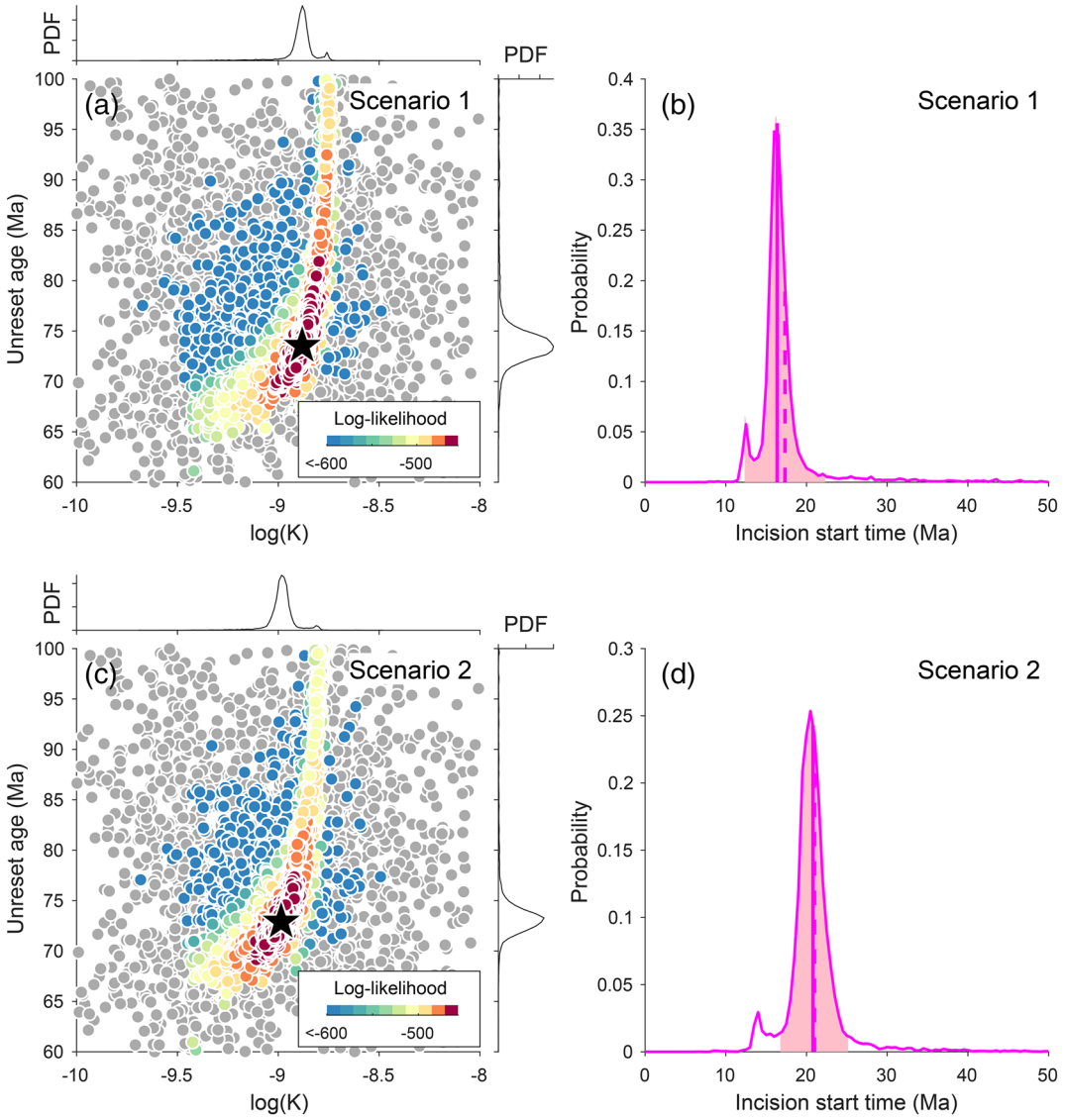

Figure 6. (a) Sampling results of the values of the erodibility *K* and the unreset (U-Th)/He age for Scenario 1. Colored dots represent forward models in the postburn-in ensemble, color-coded according to their log-likelihood, and gray the burn-in. Star indicates the "best-fit" model. Probability Density Functions (PDF) of the two parameters are plotted along the axes. (b) PDF of the incision onset time for Scenario 1 according to the sampled *K* values. Solid vertical line indicates the "best-fit" model, whereas dashed line and the shading indicate the mean and the 1-σ range, respectively. Panels (c and d) are the results for Scenario 2.

value inferred from the model of Letian Brook also applies for incision models of Baisui and Hengxi Brooks (Figure 4a and 4c), the erosion rates of the two rivers after the onset of gorge incision are variable, but generally within the ranges of 0.02–0.08 and 0.01–0.1 km/Myr, respectively. In the Hengxi Brook, the increased incision rates have eroded rocks of ~900 m-thick near the mainstem Yangtze River.

Our estimated erosion models predict an average cooling rate of <0.5°C/Myr for the Huangling Granite during the Cenozoic. This is consistent with the previous thermal history models constrained only by AFT and AHe data (Figure 8; Ge et al., 2013; Richardson et al., 2010), which suggest that the rocks have cooled from ~80°–60°C to the surface temperature during the Cenozoic. However, due to the insensitivity of the data to evolution at lower temperatures (<60°C), the previous thermal history models provided little constraints on the rock cooling processes within the final 2 km in the crust. In contrast, combining the thermochronological data with river profile analysis allows us to reveal the rock exhumation process at

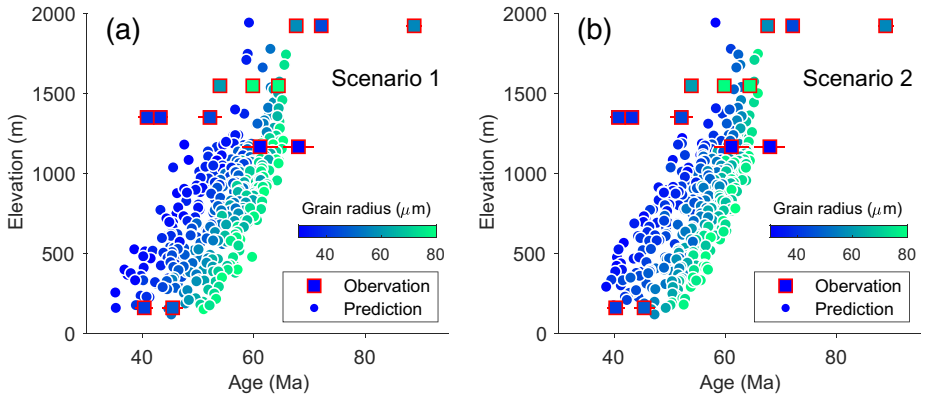

Figure 7. (a) Age versus elevation relationship of the observed (U-Th)/He ages (Hu et al., 2006; Richardson et al., 2010) and the predicted ages by the best-fit model of Scenario 1. Predicted ages shown here are using variable grain sizes at every km^2 in the catchment of Letian Brook. (b) Same as (a) but predicted ages are by the best-fit model of Scenario 2.

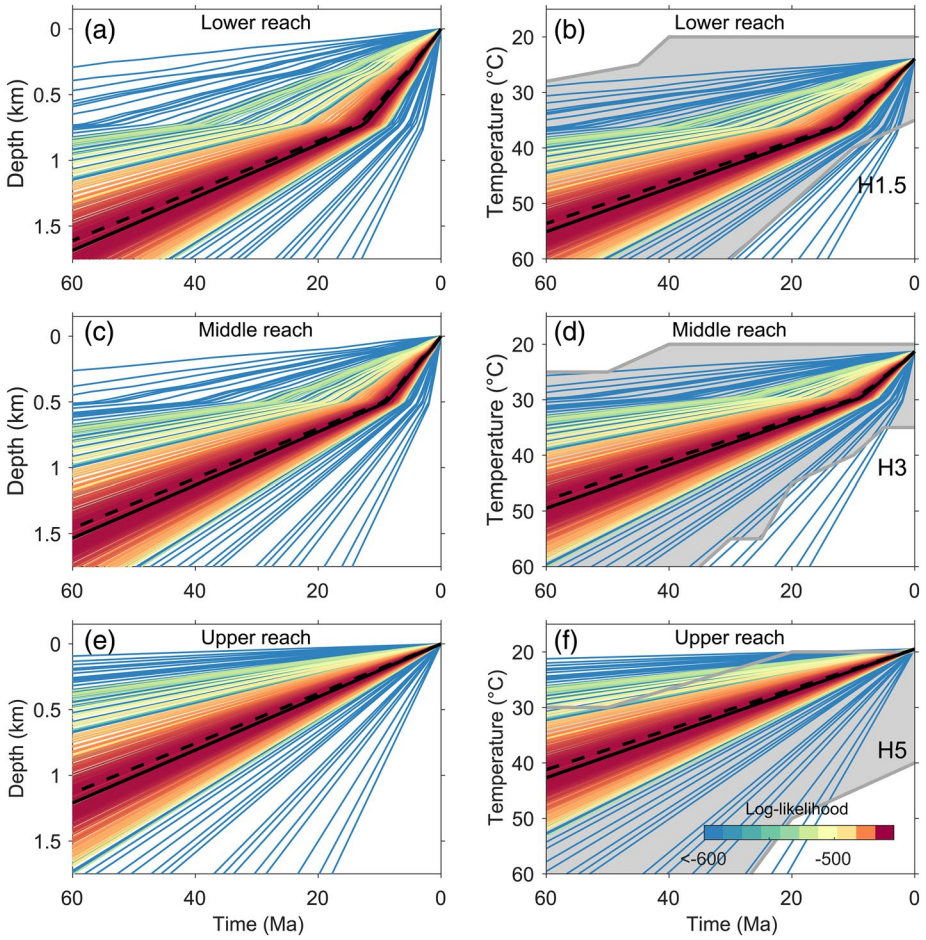

Figure 8. (left) Exhumation and (right) cooling histories for rocks at (a) and (b) lower, (c) and (d) middle, and (e) and (f) upper reaches of Letian Brook, predicted by models in Scenario 1. Results by models in Scenario 2 are very similar and thus are not shown here. Individual forward models are drawn from the postburn-in ensemble and color-coded according to their log-likelihood. Solid and dashed lines indicate the "best-fit" and mean postburn-in models, respectively. Gray lines and shaded areas show the thermal histories modeled by Richardson et al. (2010) using apatite fission track data; H1.5, H3, and H5 are samples numbers in Richardson et al. (2010).

shallower depths of the crust. Specifically in this study, increased incision rates may have caused a change in the rock cooling rates at temperatures between 30°C and 40°C (Figure 8b and 8d), which cannot be recorded by the current AHe data from the surface samples.

5.2. Possible Mechanisms for the Incision of the Three Gorges

The two scenarios of river channel paleo-topography can represent different mechanisms that led to the incision of Three Gorges. In Scenario 1, the gorge incision was driven by lowering of the base level at the mainstem Yangtze River relative to the fixed elevation of the headwater planation surface, which could be caused by different geological or geomorphic events. One possible event that could have led to the lowering of the Yangtze River bed is a large-scale reorganization of the Upper Yangtze drainage system (as proposed by Clark et al., 2004; Richardson et al., 2010; Zheng et al., 2013). Capturing the drainage area from the Upper Yangtze River would lead to a significant increase in the discharge and thus the erosive power of the river channel in the Three Gorges region. It is worth noting that the estimated incision onset of the Three Gorges is a minimum constraint for the connection between the Sichuan Basin and the Middle Yangtze River, as the capture of Upper Yangtze could be progressive (Richardson et al., 2008; Wang et al., 2014) and the most important discharge increase might be caused by a capture event upstream from the Three Gorges (e.g., Wang et al., 2013). In this case, our estimate of the gorge incision, which follows the connection between the Upper and Middle Yangtze River, is consistent with sedimentary records in the downstream Jianghan Basin (Figure 1). Between the middle Eocene and the early Oligocene, halite and salt-bearing sediments in the deposition suggest a saline lake setting for the basin (Huang & Hinnov, 2014), which suggested no freshwater input from large rivers until at least ~36.5 Ma. Based on zircon U-Pb dating of gravels in the Lower Yangtze River, Zheng et al. (2013) observed a similar pattern between source regions of the Early Miocene and the modern Yangtze River sediments, suggesting that the river was flowing through the Three Gorges since the Oligocene-Miocene boundary (~23 Ma).

If no reversal of the Upper Yangtze River occurred during the late Cenozoic, another potential mechanism for the incision of the Three Gorges would be a base level fall in the Jianghan Basin. Following uplift and exhumation during the Mesozoic, the basin changed to an extensional setting and became a deposition center during the Cretaceous, and for most part of the basin, the deposition continued throughout the Cenozoic (Zhao et al., 2010). Therefore, no basin-wide evacuation could have occurred in the Jianghan Basin during the Cenozoic, so we exclude it as a possible cause for the incision of Three Gorges.

Our Scenario 2 assumes a local uplift of the Huangling Granite relative to a fixed base level, which could be linked to the base level of either the Jianghan or Sichuan Basin, and therefore does not require a capture of the Upper Yangtze drainage area. Along the northern and northeastern margins of the Sichuan Basin, increased uplift rates during the Cenozoic have been reported perhaps due to the eastward growth of the Tibetan Plateau (Tian et al., 2012). However, it is unclear if such deformation caused by plateau growth can propagate further east to the eastern margin of the Sichuan Basin, which otherwise is in a tectonically stable region. Inversions of the Global Positioning System (GPS) data collected for the past over 2 decades (Rui & Stamps, 2019; Wang & Shen, 2020) suggest high- and moderate-deformation rates on the western and northern margins of the Sichuan Basin, respectively, whereas the strain rates to the east and south of the basin are insignificant. Therefore, we doubt that the Three Gorges could have experienced a tectonic uplift of the same order of magnitude as that in the northern margin of the Sichuan Basin (Tian et al., 2012). Alternatively, Wang et al. (2014) suggested that uplift of the Huangling Granite during the Cenozoic was a flexural rebound in response to the erosional unloading in the Three Gorges. We agree with their interpretation, and consider the incision of Three Gorges as the cause rather than the consequence of the Huangling uplift, which may induce a positive feedback to enhance the deep gorge incision.

5.3. Potential Connections of the Three Gorge Incision to the Eastern Tibetan Denudation and Regional Climate

The onset of enhanced incision of the Three Gorges is coincident with the initiation of rapid incision of the Yangtze River and its major tributaries (e.g., the Dadu and Yalong Rivers) on the eastern margin of the

Tibetan Plateau. Along the mainstem Upper Yangtze River near the First Bend, an earlier Cenozoic denudation event occurred prior to 20 Ma (Cao et al., 2019; Shen et al., 2016), whereas the last phase of rapid incision started at ~18–15 Ma (Gourbet et al., 2019; McPhillips et al., 2016). Along the tributaries, rapid incision started at ~13–10 Ma along the Dadu River (Clark et al., 2005; Ouimet et al., 2010; Tian et al., 2015; Yang et al., 2020) and ~17–14 Ma along the Yalong River (Ouimet et al., 2010; Zhang et al., 2016). These rapid incision events most likely reflect the adjustment of the river channels in response to the topographic growth of the eastern margin of the Tibetan Plateau (Wang et al., 2012). The Miocene rapid incision in the Upper Yangtze River and its tributaries are coeval with our estimate of the onset of incision of the Three Gorges (18 ± 6 Ma). Therefore, based on this temporal link, we consider that the initial incision of the Three Gorges was part of the drainage network evolution of the Upper Yangtze during the early to mid-Miocene consequent on the uplift of the eastern Tibetan Plateau, despite that mechanism linking the plateau uplift and the Upper Yangtze reorganization remains enigmatic.

The modeled histories of all three rivers predict a decrease in the incision rate starting between $t^* = 15$ and $t^* = 10$, except that the model of the Letian Brook is disrupted by a dam located at ~9 km upstream from the mainstem Yangtze (Figure 3a). Calibrating of the incision models using the best-fit K values indicates that this decrease in the incision rate has occurred since ~5–3 Ma. This is coincident with the Pliocene aridification in the East Asia, which marked a significant reduction in the annual precipitation (Farnsworth et al., 2019; Wang et al., 2019). The long-term drying trend of the climate in the drainage area of the Yangtze River has been recorded by the sporopollen records from the Lower Yangtze delta (Zhang et al., 2013). The reduced monsoonal rainfall during this period likely led to a significant drop in the water and sediment discharge from the Upper Yangtze River, and therefore has decreased the rate of gorge incision in the Three Gorges area. For the three tributaries on the Yangtze River studied in this study, the slower gorge incision rate represents as a lower rate of the base level fall, which could have been recorded by the shapes of the channel profiles.

6. Conclusions

We estimated the incision history of the eastern Three Gorges, based on inverse modeling of the channel profiles of three tributaries of the Yangtze River and the previously reported apatite (U-Th)/He data from one of the tributary catchments. Using a low-relief planation surface as a marker of the preincision topography, our models suggest that downcutting of the Three Gorges started during the early Miocene. Although the current data do not allow us to distinguish whether the gorge incision was driven by local tectonic uplift or a capture of the modern Upper Yangtze by the Middle Yangtze, we infer that the latter is more consistent with the relatively stable tectonic setting of the eastern margin of the Sichuan Basin. Our estimated onset of the incision of the Three Gorges is coincident with the significant denudation of the eastern Tibetan Plateau, suggesting that the early to mid-Miocene is an important period in shaping the modern Upper Yangtze River. Our models also predict a marked decrease in the gorge incision rate since the Pliocene, which was probably driven by the continuous drying of the East Asia.

Data Availability Statement

Thermochronological data used in this study were published by Hu et al. (2006) and Richardson et al. (2010). TopoToolBox 2 (Schwanghart & Scherler, 2014) was used for manipulating topographic data. A MATLAB implementation of the ensemble sampler (github.com/grinsted/gwmcmc) was used for MCMC sampling.

Acknowledgments
Jiao received support from the Natural Sciences and Engineering Research Council of Canada (Discovery Grant 2019–00,243). Yang's contribution was funded by the National Natural Science Foundation of China (41961134031). We thank Amy East and three anonymous reviewers, whose comments and suggestions helped improve the paper significantly.

References

An, Z., Kutzbach, J. E., Prell, W. L., & Porter, S. C. (2001). Evolution of Asian monsoons and phased uplift of the Himalaya–Tibetan plateau since Late Miocene times. *Nature*, *411*(6833), 62–66. https://doi.org/10.1038/35075035

Armitage, J. J., Dunkley Jones, T., Duller, R. A., Whittaker, A. C., & Allen, P. A. (2013). Temporal buffering of climate-driven sediment flux cycles by transient catchment response. *Earth and Planetary Science Letters*, *369–370*, 200–210. https://doi.org/10.1016/j.epsl.2013.03.020

Braun, J., & Robert, X. (2005). Constraints on the rate of post-orogenic erosional decay from low-temperature thermochronological data: Application to the Dabie Shan, China. *Earth Surface Processes and Landforms*, *30*(9), 1203–1225. https://doi.org/10.1002/esp.1271

Braun, J., van der Beek, P., Valla, P., Robert, X., Herman, F., Glotzbach, C., et al. (2012). Quantifying rates of landscape evolution and tectonic processes by thermochronology and numerical modeling of crustal heat transport using PECUBE. *Tectonophysics*, *524–525*, 1–28. https://doi.org/10.1016/j.tecto.2011.12.035

Cao, K., Wang, G., Leloup, P. H., Mahéo, G., Xu, Y., van der Beek, P. A., et al. (2019). Oligocene-Early Miocene topographic relief generation of southeastern Tibet triggered by thrusting. *Tectonics*, *38*(1), 374–391. https://doi.org/10.1029/2017TC004832

Clark, M. K., House, M. A., Royden, L. H., Whipple, K. X., Burchfiel, B. C., Zhang, X., et al. (2005). Late Cenozoic uplift of southeastern Tibet. *Geology*, *33*(6), 525–528. https://doi.org/10.1130/G21265.1

Clark, M. K., Schoenbohm, L. M., Royden, L. H., Whipple, K. X., Burchfiel, B. C., Zhang, X., et al. (2004). Surface uplift, tectonics, and erosion of eastern Tibet from large-scale drainage patterns. *Tectonics*, *23*(1), 1–21. https://doi.org/10.1029/2002TC001402

Clift, P. D., Blusztajn, J., & Nguyen, A. D. (2006). Large-scale drainage capture and surface uplift in eastern Tibet–SW China before 24 Ma inferred from sediments of the Hanoi Basin, Vietnam. *Geophysical Research Letters*, *33*(19), L19403. https://doi.org/10.1029/2006GL027772

Ding, Y. (1992). Summer Monsoon Rainfalls in China. *Journal of the Meteorological Society of Japan. Ser. II*, *70*(1B), 373–396. https://doi.org/10.2151/jmsj1965.70.1B_373

Dong, Y., & Santosh, M. (2016). Tectonic architecture and multiple orogeny of the Qinling Orogenic Belt, Central China. *Gondwana Research*, *29*(1), 1–40. https://doi.org/10.1016/j.gr.2015.06.009

Farley, K. A. (2000). Helium diffusion from apatite: General behavior as illustrated by Durango fluorapatite. *Journal of Geophysical Research*, *105*(B2), 2903–2914. https://doi.org/10.1029/1999JB900348

Farnsworth, A., Lunt, D. J., Robinson, S. A., Valdes, P. J., Roberts, W. H. G., Clift, P. D., et al. (2019). Past East Asian monsoon evolution controlled by paleogeography, not CO_2. *Science Advances*, *5*(10), eaax1697. https://doi.org/10.1126/sciadv.aax1697

Feng, J., & Cui, Z. (2002). The reconstruction of fossil planation surface in China. *Chinese Science Bulletin*, *47*(5), 434. https://doi.org/10.1360/02tb9101

Fox, M. (2019). A linear inverse method to reconstruct paleo-topography. *Geomorphology*, *337*, 151–164. https://doi.org/10.1016/j.geomorph.2019.03.034

Fox, M., Bodin, T., & Shuster, D. L. (2015). Abrupt changes in the rate of Andean Plateau uplift from reversible jump Markov Chain Monte Carlo inversion of river profiles. *Geomorphology*, *238*, 1–14. https://doi.org/10.1016/j.geomorph.2015.02.022

Gao, S., Yang, J., Zhou, L., Li, M., Hu, Z., Guo, J., et al. (2011). Age and growth of the Archean Kongling terrain, South China, with emphasis on 3.3 GA granitoid gneisses. *American Journal of Science*, *311*(2), 153–182. https://doi.org/10.2475/02.2011.03

Ge, X., Shen, C., Yang, Z., Mei, L., Xu, S., Peng, L., et al. (2013). Low-temperature thermochronology constraints on the mesozoic-cenozoic exhumation of the Huangling massif in the Middle Yangtze Block, Central China. *Journal of Earth Science*, *24*(4), 541–552. https://doi.org/10.1007/s12583-013-0348-8

Goodman, J., & Weare, J. (2010). Ensemble samplers with affine invariance. *Communications in Applied Mathematics and Computational Science*, *5*(1), 65–80. https://doi.org/10.2140/camcos.2010.5.65

Goren, L. (2016). A theoretical model for fluvial channel response time during time-dependent climatic and tectonic forcing and its inverse applications. *Geophysical Research Letters*, *43*(20753–10), 10. https://doi.org/10.1002/2016GL070451

Goren, L., Fox, M., & Willett, S. D. (2014). Tectonics from fluvial topography using formal linear inversion: Theory and applications to the Inyo Mountains, California. *Journal of Geophysical Research*, *119*(8), 1651–1681. https://doi.org/10.1002/2014JF003079

Gourbet, L., Yang, R., Fellin, M. G., Paquette, J.-L., Willett, S. D., Gong, J., et al. (2019). Evolution of the Yangtze River network, southeastern Tibet: Insights from thermochronology and sedimentology. *Lithosphere*, *12*(1), 3–18. https://doi.org/10.1130/L1104.1

Guillocheau, F., Simon, B., Baby, G., Bessin, P., Robin, C., & Dauteuil, O. (2018). Planation surfaces as a record of mantle dynamics: The case example of Africa. *Gondwana Research*, *53*, 82–98. https://doi.org/10.1016/j.gr.2017.05.015

Howard, A. D., & Kerby, G. (1983). Channel changes in badlands. *Geological Society of America Bulletin*, *94*(6), 739–752. https://doi.org/10.1130/0016-7606(1983)94<739:CCIB>2.0.CO;2

Huang, C., & Hinnov, L. (2014). Evolution of an Eocene-Oligocene saline lake depositional system and its controlling factors, Jianghan Basin, China. *Journal of Earth Science*, *25*(6), 959–976. https://doi.org/10.1007/s12583-014-0499-2

Hu, S., Raza, A., Min, K., Kohn, B. P., Reiners, P. W., Ketcham, R. A., et al. (2006). Late Mesozoic and Cenozoic thermotectonic evolution along a transect from the north China craton through the Qinling orogen into the Yangtze craton, central China. *Tectonics*, *25*(6), TC6009. https://doi.org/10.1029/2006TC001985

Li, S., Jahn, B.-M., Zhao, S., Dai, L., Li, X., Suo, Y., et al. (2017). Triassic southeastward subduction of North China Block to South China Block: Insights from new geological, geophysical and geochemical data. *Earth-Science Reviews*, *166*, 270–285. https://doi.org/10.1016/j.earscirev.2017.01.009

Li, S., Santosh, M., Zhao, G., Zhang, G., & Jin, C. (2012). Intracontinental deformation in a Frontier of super-convergence: A perspective on the tectonic milieu of the South China Block. *Journal of Asian Earth Sciences*, *49*, 313–329. https://doi.org/10.1016/j.jseaes.2011.07.026

Li, J., Xie, S., & Kuang, M. (2001). Geomorphic evolution of the Yangtze Gorges and the time of their formation. *Geomorphology*, *41*(2–3), 125–135. https://doi.org/10.1016/S0169-555X(01)00110-6

Li, X., Zhang, H., Wang, Y., Zhao, X., Ma, Z., Liu, K., et al. (2020). Inversion of bedrock channel profiles in the Daqing Shan in Inner Mongolia, northern China: Implications for late Cenozoic tectonic history in the Hetao Basin and the Yellow River evolution. *Tectonophysics*, *790*, 228558. https://doi.org/10.1016/j.tecto.2020.228558

McPhillips, D., Hoke, G. D., Liu-Zeng, J., Bierman, P. R., Rood, D. H., & Niedermann, S. (2016). Dating the incision of the Yangtze River gorge at the First Bend using three-nuclide burial ages. *Geophysical Research Letters*, *43*(1), 101–110. https://doi.org/10.1002/2015GL066780

Orme, A. (2013). *Denudation, Planation, and Cyclicity: Myths, Models, and Reality*. In A. R. Orme, & D. Sack (Eds.), The foundations of geomorphology. Vol. 1 (pp. 205–232). https://doi.org/10.1016/B978-0-12-374739-6.00012-9

Ouimet, W., Whipple, K., Royden, L., Reiners, P., Hodges, K., & Pringle, M. (2010). Regional incision of the eastern margin of the Tibetan Plateau. *Lithosphere*, *2*(1), 50–63. https://doi.org/10.1130/L57.1

Perron, J. T., & Royden, L. (2013). An integral approach to bedrock river profile analysis. *Earth Surface Processes and Landforms*, *38*(6), 570–576. https://doi.org/10.1002/esp.3302

Rao, Y., Liu, X., Fu, Y., Meng, H., & Li, J. (2013). Planation surfaces of eastern Dabie Mountains, China. *Journal of Geodesy and Geodynamics*, *33*(6), 62–67.

Reiners, P. W., Zhou, Z., Ehlers, T. A., Xu, C., Brandon, M. T., Donelick, R. A., et al. (2003). Post-orogenic evolution of the Dabie Shan, eastern China, from (U-Th)/He and fission-track thermochronology. *American Journal of Science*, *303*(6), 489–518. https://doi.org/10.2475/ajs.303.6.489

Richardson, N. J., Densmore, A. L., Seward, D., Fowler, A., Wipf, M., Ellis, M. A., et al. (2008). Extraordinary denudation in the Sichuan Basin: Insights from low-temperature thermochronology adjacent to the eastern margin of the Tibetan Plateau. *Journal of Geophysical Research*, *113*(B4), B04409. https://doi.org/10.1029/2006JB004739

Richardson, N. J., Densmore, A. L., Seward, D., Wipf, M., & Yong, L. (2010). Did incision of the Three Gorges begin in the Eocene? *Geology*, *38*(6), 551–554. https://doi.org/10.1130/G30527.1

Rowley, D. B., & Currie, B. S. (2006). Palaeo-altimetry of the late Eocene to Miocene Lunpola basin, central Tibet. *Nature*, *439*(7077), 677–681. https://doi.org/10.1038/nature04506

Royden, L., & Perron, J. T. (2013). Solutions of the stream power equation and application to the evolution of river longitudinal profiles. *Journal of Geophysical Research: Earth Surface*, *118*(2), 497–518. https://doi.org/10.1002/jgrf.20031

Rui, X., & Stamps, D. S. (2019). A geodetic strain rate and tectonic velocity model for China. *Geochemistry, Geophysics, Geosystems*, *20*(3), 1280–1297. https://doi.org/10.1029/2018GC007806

Schwanghart, W., & Scherler, D. (2014). Short Communication: TopoToolbox 2 - MATLAB-based software for topographic analysis and modeling in Earth surface sciences. *Earth Surface Dynamics*, *2*(1), 1–7. https://doi.org/10.5194/esurf-2-1-2014

Shen, Y. (1965). *The valley landform of the upper Yangtze (in Chinese)*. Beijing.

Shen, C., Mei, L., Peng, L., Chen, Y., Yang, Z., & Hong, G. (2012). LA-ICPMS U–Pb zircon age constraints on the provenance of Cretaceous sediments in the Yichang area of the Jianghan Basin, central China. *Cretaceous Research*, *34*, 172–183. https://doi.org/10.1016/j.cretres.2011.10.016

Shen, X., Tian, Y., Li, D., Qin, S., Vermeesch, P., & Schwanethal, J. (2016). Oligocene-Early Miocene river incision near the first bend of the Yangze River: Insights from apatite (U-Th-Sm)/He thermochronology. *Tectonophysics*, *687*, 223–231. https://doi.org/10.1016/j.tecto.2016.08.006

Shi, W., Dong, S.-W., Ratschbacher, L., Tian, M., Li, J.-H., & Wu, G.-L. (2013). Meso-Cenozoic tectonic evolution of the Dangyang Basin, north-central Yangtze craton, central China. *International Geology Review*, *55*(3), 382–396. https://doi.org/10.1080/00206814.2012.715732

Sun, X., & Wang, P. (2005). How old is the Asian monsoon system?—Palaeobotanical records from China. *Palaeogeography, Palaeoclimatology, Palaeoecology*, *222*(3–4), 181–222. https://doi.org/10.1016/j.palaeo.2005.03.005

Tian, Y., Kohn, B. P., Hu, S., & Gleadow, A. J. W. (2015). Synchronous fluvial response to surface uplift in the eastern Tibetan Plateau: Implications for crustal dynamics. *Geophysical Research Letters*, *42*(1), 29–35. https://doi.org/10.1002/2014GL062383

Tian, Y., Kohn, B. P., Zhu, C., Xu, M., Hu, S., & Gleadow, A. J. W. (2012). Post-orogenic evolution of the Mesozoic Micang Shan Foreland Basin system, central China. *Basin Research*, *24*(1), 70–90. https://doi.org/10.1111/j.1365-2117.2011.00516.x

Wang, E., Kirby, E., Furlong, K. P., Van Soest, M., Xu, G., Shi, X., et al. (2012). Two-phase growth of high topography in eastern Tibet during the Cenozoic. *Nature Geoscience*, *5*(9), 640–645. https://doi.org/10.1038/ngeo1538

Wang, H., Lu, H., Zhao, L., Zhang, H., Lei, F., & Wang, Y. (2019). Asian monsoon rainfall variation during the Pliocene forced by global temperature change. *Nature Communications*, *10*(1), 5272. https://doi.org/10.1038/s41467-019-13338-4

Wang, E., Meng, Q., Burchfiel, B. C., & Zhang, G. (2003). Mesozoic large-scale lateral extrusion, rotation, and uplift of the Tongbai-Dabie Shan belt in East China. *Geology*, *31*(4), 307–310. https://doi.org/10.1130/0091-7613(2003)031<0307:MLSLER>2.0.CO;2

Wang, M., & Shen, Z. (2020). Present-day crustal deformation of continental China derived from GPS and its tectonic implications. *Journal of Geophysical Research: Solid Earth*, *125*(2), e2019JB018774. https://doi.org/10.1029/2019JB018774

Wang, C., Zhao, X., Liu, Z., Lippert, P. C., Graham, S. A., Coe, R. S., et al. (2008). Constraints on the early uplift history of the Tibetan Plateau. *Proceedings of the National Academy of Sciences of the United States of America*, *105*(13), 4987–4992. https://doi.org/10.1073/pnas.0703595105

Wang, P., Zheng, H., Chen, L., Chen, J., Xu, Y., Wei, X., et al. (2014). Exhumation of the Huangling anticline in the Three Gorges region: Cenozoic sedimentary record from the western Jianghan Basin, China. *Basin Research*, *26*(4), 505–522. https://doi.org/10.1111/bre.12047

Wang, P., Zheng, H., & Liu, S. (2013). Geomorphic constraints on Middle Yangtze River reversal in eastern Sichuan Basin, China. *Journal of Asian Earth Sciences*, *69*, 70–85. https://doi.org/10.1016/j.jseaes.2012.09.018

Wei, Y., Peng, S., Jiang, X., Peng, Z., Peng, L., Li, Z., et al. (2012). SHRIMP zircon U-Pb ages and geochemical characteristics of the neoproterozoic granitoids in the Huangling anticline and its tectonic setting. *Journal of Earth Science*, *23*(5), 659–676. https://doi.org/10.1007/s12583-012-0284-z

Whipple, K. X., & Tucker, G. E. (1999). Dynamics of the stream-power river incision model: Implications for height limits of mountain ranges, landscape response timescales, and research needs. *Journal of Geophysical Research*, *104*(B8), 17661–17674. https://doi.org/10.1029/1999JB900120

Xiang, F., Zhu, L., Wang, C., Zhao, X., Chen, H., & Yang, W. (2007). Quaternary sediment in the Yichang area: Implications for the formation of the Three Gorges of the Yangtze River. *Geomorphology*, *85*(3–4), 249–258. https://doi.org/10.1016/j.geomorph.2006.03.027

Xie, S., Yuan, D., Wang, J., & Kuang, M. (2006). Features of the planation surface in the surrounding area of the Three Gorges of Yangtze. *Carsologica Sinica*, *25*(1), 40–45.

Yang, Z., Shen, C., Ratschbacher, L., Enkelmann, E., Jonckheere, R., Wauschkuhn, B., et al. (2017). Sichuan Basin and beyond: Eastward foreland growth of the Tibetan Plateau from an integration of Late Cretaceous-Cenozoic fission track and (U-Th)/He ages of the eastern Tibetan Plateau, Qinling, and Daba Shan. *Journal of Geophysical Research: Solid Earth*, *122*(6), 4712–4740. https://doi.org/10.1002/2016JB013751

Yang, R., Suhail, H. A., Gourbet, L., Willett, S. D., Fellin, M. G., Lin, X., et al. (2020). Early Pleistocene drainage pattern changes in Eastern Tibet: Constraints from provenance analysis, thermochronometry, and numerical modeling. *Earth and Planetary Science Letters*, *531*, 115955. https://doi.org/10.1016/j.epsl.2019.115955

Yuan, Y.-S., Ma, Y.-S., Hu, S.-B., Guo, T.-L., & Fu, X.-Y. (2006). Present-Day Geothermal Characteristics in South China. *Chinese Journal of Geophysics*, *49*(4), 1005–1014. https://doi.org/10.1002/cjg2.922

Zhang, K. (2008). Planation surfaces in China: One hundred years of investigation. *Geological Society, London, Special Publications*, *301*(1), 171–178. https://doi.org/10.1144/SP301.12

Zhang, G., Meng, Q., Yu, Z., Sun, Y., Zhou, D., & Guo, A. (1996). Orogenesis and dynamics of the Qinling orogen. *Science in China - Series D*, *39*(3), 685. https://doi.org/10.1360/yd1996-39-3-225

Zhang, P., Miao, Y., Zhang, Z., Lu, S., Zhang, Y., Chen, H., et al. (2013). Late Cenozoic sporopollen records in the Yangtze River Delta, East China and implications for East Asian summer monsoon evolution. *Palaeogeography, Palaeoclimatology, Palaeoecology*, *388*, 153–165. https://doi.org/10.1016/j.palaeo.2013.08.014

Zhang, H., Oskin, M. E., Liu-Zeng, J., Zhang, P., Reiners, P. W., & Xiao, P. (2016). Pulsed exhumation of interior eastern Tibet: Implications for relief generation mechanisms and the origin of high-elevation planation surfaces. *Earth and Planetary Science Letters*, *449*, 176–185. https://doi.org/10.1016/j.epsl.2016.05.048

Zhao, C.-Y., Song, H.-B., Qian, R.-Y., Song, Y., Huang, X.-H., Chen, L., et al. (2010). Research on tectono-thermal evolution modeling method for superimposed basin with the Jianghan Basin as an example. *Chinese Journal of Geophysics*, *53*(1), 92–102. https://doi.org/10.1002/cjg2.1476

Zheng, H. (2015). Birth of the Yangtze River: Age and tectonic-geomorphic implications. *National Science Review*, *2*(4), 438–453. https://doi.org/10.1093/nsr/nwv063

Zheng, H., Clift, P. D., Wang, P., Tada, R., Jia, J., He, M., et al. (2013). Pre-Miocene birth of the Yangtze River. *Proceedings of the National Academy of Sciences*, *110*(19), 7556–7561. https://doi.org/10.1073/pnas.1216241110